JOURNAL OF CATALYSIS 67, 316–323 (1981)

Catalysis of *n*-Butane Conversion by Aluminum Chloride in Molten Salt Mixtures

YASUO OHTSUKA AND YASUKATSU TAMAI

Chemical Research Institute of Non-Aqueous Solutions, Tohoku University, Katahira, Sendai 980, Japan

Received April 21, 1980; revised August 27, 1980

Catalytic behavior of molten salts containing aluminum chloride for *n*-butane conversion was investigated in a flow reactor at temperatures ranging from 100 to 165°C under atmospheric pressure. Main products were propane and isobutane, and a slight amount of 2-methyl butane was also obtained. The overall reaction rate was expressed by the equation $k[A + K_{HCl}P_{HCl}/(1 + K_{HCl}P_{HCl})]P_{n-B}$, which was derived by assuming that the formation of a carbonium ion on the melt surface is the rate-controlling step. The overall reaction rate had a maximum in the plots of rate against temperature, and this phenomenon was explained by the change of surface concentration of HCl with temperature. Furthermore it was found that the catalytic activity changed smoothly on supercooling of the eutectic melt of $AlCl_3$ and NaCl but decreased drastically on the phase transition from the molten to the solid state. The difference in catalytic activity between the two states is discussed in terms of structural changes of the aluminum chloride.

INTRODUCTION

In recent years several significant characteristics of molten salt catalysts have attracted increasing attention (*1*) and there are many patents and publications on their practical applications, particularly in clorination of hydrocarbons (*2, 3*), and gasification (*4, 5*) and hydroliquefaction (*6, 7*) of coal. However, only a few studies have been made to clarify the role of molten salts in catalytic reactions of organic compounds (*8–11*).

We now wish to report the catalytic behavior of molten salts containing aluminum chloride for *n*-butane conversion. Solid aluminum chloride is one of the most important Lewis acid catalysts and its structure changes drastically on melting (*12*). Therefore it is of considerable interest to investigate the effect of the pronounced structural changes on catalytic activity for a Friedel–Crafts reaction such as *n*-butane isomerization. Isomerization of saturated hydrocarbons catalyzed by Lewis acid halides is a process of academic interest as well as of practical importance in the petroleum refinery. Hence, the process has been studied by various methods, but there has been no study on the reaction mechanism with molten salt catalysts.

The main purpose of this work is to clarify the role of molten aluminum chloride in the catalytic conversion of *n*-butane by changing the reaction temperature, the feed gas composition, and the salt composition. Also there is a great interest in examining the difference in catalytic activity of the salt between the molten and the solid states. Only one paper on this topic for Lewis acid-catalyzed reactions has been published—that of Kenney and Takahashi (*9*). Their finding was a smooth change in rate at the melting point of zinc chloride for dehydrochlorination of isopropyl chloride.

EXPERIMENTAL

Apparatus

Figure 1 shows a flow reactor system made of Pyrex glass. A small shallow boat, placed horizontally in a tubular reactor, served as a container for the molten catalyst. The reactor was connected directly to

0021-9517/81/020316-08$02.00/0

the preparation vessel of the catalyst through greaseless tubing to avoid moisture. The reactor tube was heated electrically by nichrome wire and insulated thermally by an annular Pyrex tube. This assembly made it possible to observe directly any change in appearance of the catalyst. The reaction temperature was kept constant within ±2 K along the boat.

Materials

$AlCl_3$, LiCl, and NaCl were commercial reagents of guaranteed grade and they were used as received. The reactant gas consisted of n-C_4H_{10}, HCl, and He diluent, which were of research grade. Both silica gel and molecular sieve 5A were used as drying agents for n-C_4H_{10} and He, and concentrated H_2SO_4 was used for HCl. The gas chromatogram of n-C_4H_{10} showed purity above 99.9% and most of the impurity was i-C_4H_{10}.

Catalyst Preparation

The powdery salt mixture of a given molar ratio was put into the preparation vessel in a dry box flushed with N_2. Then the vessel was taken out of the box and quickly connected to the reactor. After evacuation of the whole device, the vessel was heated to the melting point of the salt mixture. When the salt melted under vacuum, an atmospheric pressure of He was admitted to the vessel. He was allowed to bubble into the melt through greaseless tubing, and the melt was stirred magnetically. This agitation caused the scum in the melt to float to the upper layer. Also the impurities having higher specific gravities than that of the melt could settle down at the bottom of the vessel. Finally the pressurized helium, admitted from the top of the vessel, pushed the melt into the Pyrex boat through the connecting tube. The melt was a clear, slightly colored (very light yellow) liquid and had an apparent surface area of 50 cm^2 in the boat.

With the runs using a solid salt, the fresh melt in the boat was cooled below the melting point in flowing helium. Therefore its active surface area was equal to that of the melt. However, since the formation of cracks on the solid surface was observed by scanning electron microscope, the actual surface area was higher than that of the melt.

Experimental Condition and Procedure

The catalyst was, in most cases, a eutectic mixture (mp 110°C) of 61 mol% $AlCl_3$ and 39 mol% NaCl. Considering catalyst deterioration after a prolonged reaction, a fresh melt was charged into the boat prior to each run. The reactant gas was a mixture of 21 vol% n-C_4H_{10} and 37 vol% HCl in He diluent unless otherwise stated.

After the catalyst salt had been kept at the reaction temperature (100–165°C) for a given time in a flow of helium, the atmospheric gas mixture was introduced into the

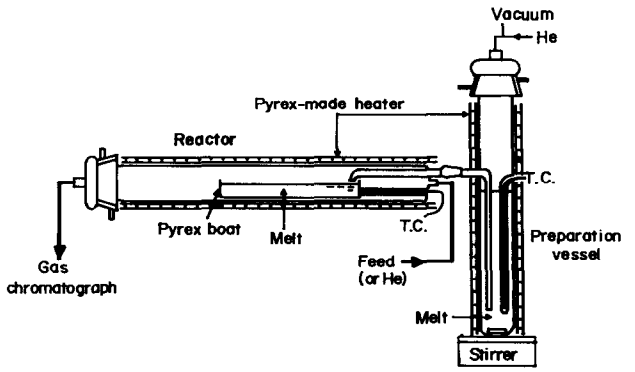

FIG. 1. Apparatus.

reactor and passed continuously over the salt at a flow rate of 61 cm³(STP)/min. The reaction time was measured from the beginning of the introduction. Reaction products were analyzed periodically by a gas chromatography, and C_3H_8, *n*- and *i*-C_4H_{10} and *i*-C_5H_{12} (2-methyl butane) were separated with a 9-m column of 30 wt% propylene carbonate on C-22. Product yields were calculated as the mole percentage of total hydrocarbon present in the gas sample.

RESULTS

Time Dependence of Product Yields

The main products were C_3H_8 and *i*-C_4H_{10}. A small amount of *i*-C_5H_{12} was also obtained but it was less than 5% of the amount of C_3H_8 formed. Figure 2 shows a typical time dependence of propane and isobutane yield. The reproducibility of the results was within ±3.5%.

The propane formation occurred after a short induction period and the rate increased until a steady state was attained. The length of the period shortened with a rise in temperature. For the isobutane formation, there was the plateau where the yield was independent of time at the beginning of the reaction. After the plateau the rate increased and finally reached a steady state. The length of the first plateau shortened as the temperature was increased. The figure shows that the isobutane formation precedes the propane formation.

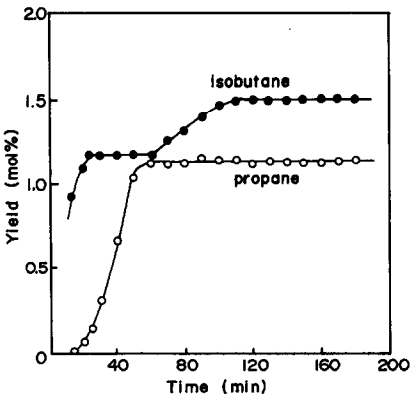

FIG. 2. Propane and isobutane yields as a function of reaction time at 135°C.

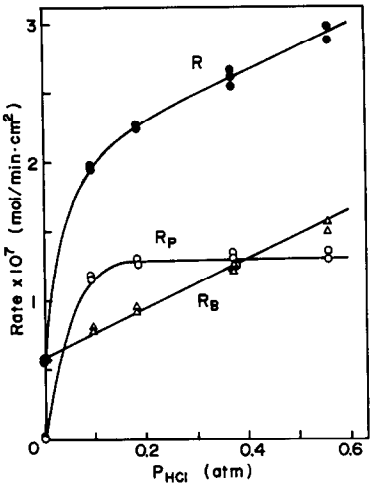

FIG. 3. Dependence of rates on P_{HCl} at 150°C.

Effect of Feed Gas Composition

In order to clarify the reaction kinetics on the molten catalyst, partial pressures of HCl (P_{HCl}) and *n*-C_4H_{10} (P_{n-B}) in the gas mixture were changed. In Fig. 3, the rates at the steady state are plotted against P_{HCl} at 150°C and 0.210 atm (1 atm = 101 kPa) of P_{n-B}. The letters, R, R_P, and R_B in the figure represent the rate of overall reaction, propane formation, and isobutane formation, respectively. Owing to the very slow rate of

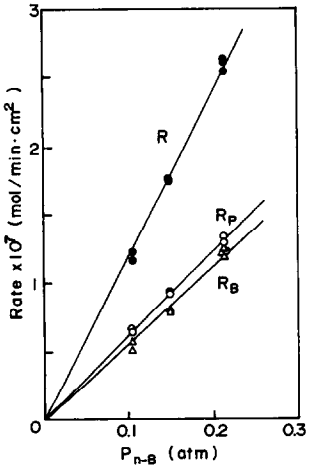

FIG. 4. Dependence of rates on P_{n-B} at 150°C.

isopentane formation, R almost equals the sum of R_P and R_B. Interestingly, in the absence of HCl, only i-C_4H_{10} was formed. R_B increased linearly with P_{HCl}, whereas R_P was independent of P_{HCl} above 0.20 atm. Figure 4 shows that R, R_P, and R_B are nearly proportional to P_{n-B} in range of 0.104 to 0.210 atm.

Effect of Melt Composition

The bulk composition of catalyst melt was changed to determine the catalytically active species. Figure 5 illustrates the dependence of rates on the concentration of $AlCl_3$ at 150°C. All rates increased linearly with the concentrations in the range of 55.0 to 67.0 mol%. A noteworthy result is that these rates approach zero at approximately 50 mol% in the concentration. This finding was confirmed by the experiments with the lower concentrations ranging from 50.5 to 55.0 mol% at the higher temperature of 190°C, although the rates gradually decreased during the experiments owing to the appreciable sublimation loss of $AlCl_3$.

As shown in Fig. 6, substituting Li^+ for Na^+ ion in the melts markedly affected the rates. Here the bulk concentration of $AlCl_3$ was kept constant at 61 mol%. R_P decreased slightly with increasing concentration of Li^+ ion but R_B increased considerably, and consequently R increased. The complete substitution of Li^+ for Na^+ ion not only doubled R but also increased the selectivity to isobutane from 47 to 74 mol%.

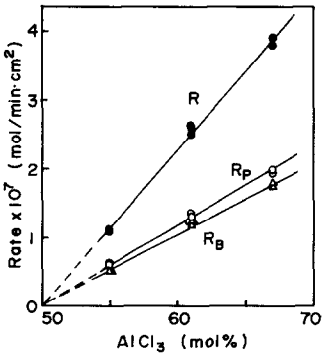

FIG. 5. Effect of concentration of $AlCl_3$ on rates at 150°C.

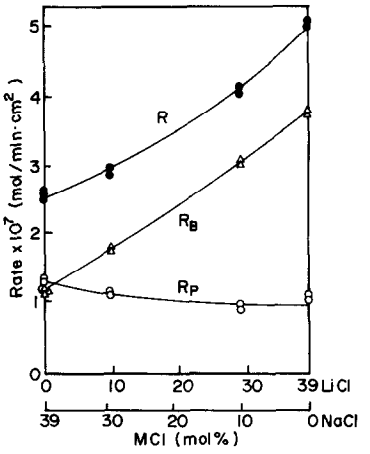

FIG. 6. Effect of Li^+ ion rates at 150°C.

Temperature Dependence

Temperature dependence of the rates is given in Fig. 7. As the catalyst salt changed from the solid state (100°C) to the molten state (115°C), R increased drastically, by a factor of about 25. The increment is in fact larger because the actual surface area is lower with the molten salt than that with the solid having cracks. In the molten state region, R, R_P, and R_B all had maxima in the plots of rate against temperature.

Catalytic Activity in a Supercooled Molten State

As no study has previously been done on the catalytic activity of the supercooled state of metal halides, some experiments were conducted on this point. The eutectic melt under reaction was cooled down carefully below its melting point, and was maintained at the supercooled state. In the meantime, owing to its instability, the supercooled melt solidified. Figure 8 illustrates a typical change of activity on solidification. As the temperature of the melt was reduced from 120 to 105°C, both propane and isobutane yields decreased. These yields in the supercooled state were in reasonable agreement with those estimated by extrapolating the data in Fig. 7 to 105°C. On solidification of the supercooled

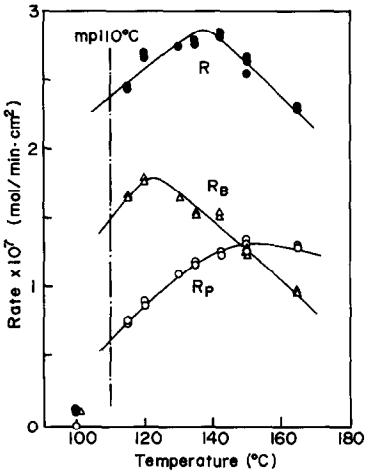

FIG. 7. Temperature dependence of rates for the eutectic salt.

melt, both yields fell rapidly to extremely small values. It took 30–40 min to reach the steady states, and the time lag may be interpreted as necessary for the completion of phase transition. It should be emphasized that the activity changes smoothly on supercooling the catalyst melt, but it decreases drastically on phase transition from the supercooled state to the solid.

DISCUSSION

Reaction Zone or Site

We will first clarify whether the reaction takes place in the gas phase, in the bulk of the melt, or on the melt surface. In Fig. 9, $1/(R - R_0)$, where R_0 is R at $P_{HCl} = 0$ atm, is plotted against $1/P_{HCl}$. The linear relationship between $1/(R - R_0)$ and $1/P_{HCl}$ means that the adsorption of HCl on the catalyst melt is of a Langmuir type, which suggests that the *n*-butane conversion proceeds predominantly on the melt surface. From the figure, R can be written as

$$R = k'\left(A + \frac{K_{HCl}P_{HCl}}{1 + K_{HCl}P_{HCl}}\right), \qquad (1)$$

where $k'A$ equals R_0, k' is the rate constant, A is the constant, and K_{HCl} is the adsorption coefficient for HCl. It has been reported that the adsorption of HCl on supported aluminum chloride catalyst is of a Langmuir type (*13*).

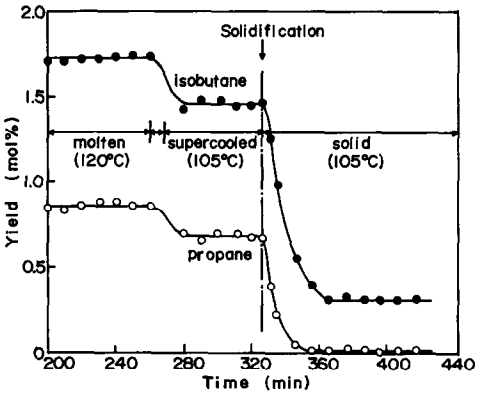

FIG. 8, Catalytic activity of a supercooled melt at 105°C and the change in the activity on solidification of the melt.

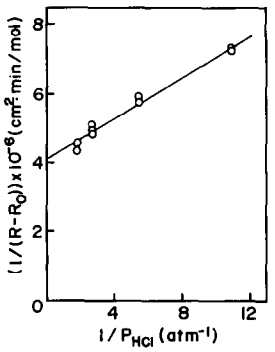

FIG. 9. A plot of $1/(R - R_0)$ versus $1/P_{HCl}$ at 150°C.

Catalytically Active Species

The species present in the bulk of the present catalyst melt have been studied by Raman spectroscopy (*14, 15*). It is well established that $AlCl_4^-$ tetrahedron ion and Al_2Cl_6 molecule are the only species at 50 and 100 mol% $AlCl_3$, respectively. The presence of $Al_2Cl_7^-$ also has been shown in the intermediate compositions, and the species may be formed by the reaction of $AlCl_4^-$ and Al_2Cl_6. As the concentration of $AlCl_3$ is increased, the relative intensity of the peak due to $AlCl_4^-$ decreases, and conversely that for Al_2Cl_6 increases. Accordingly, if the surface composition of the melt is similar to the bulk, the proportional rela-

tion between the concentration and R (Fig. 5) suggests that the catalytically active species may be dimeric Al_2Cl_6. Judging from the disappearance of the activity near 50 mol%, the species $AlCl_4^-$ is catalytically inactive.

The difference in reaction rate between Li^+ and Na^+ ion (Fig. 6) could be explained on the basis of the relative stability of the species Al_2Cl_6. Because of its stronger polarizing power, Li^+ ion has the smaller tendency toward intermolecular compound formation with the Al_2Cl_6 molecule. This is evident from the higher vapor pressure of aluminum chloride for $LiCl$–$AlCl_3$ (*17*) compared to that for $NaCl$–$AlCl_3$ (*18*). In the melts containing Li^+ ion, therefore, Al_2Cl_6 is more stable and predominant (*15*). As a result, the substitution of Li^+ ion for Na^+ ion enhanced the overall reaction rate (R), as shown in Fig. 6. Such an effect of alkali metal cation on catalytic activity has been observed also for dehydrochlorination of isopropyl chloride catalyzed by molten zinc chloride (*9*). The higher selectivity for isobutane with the melts containing Li^+ ion is a very interesting result, but is not explicable in terms of the above discussion. Hence other possibilities should be examined by considering the process of C_3H_8 and i-C_4H_{10} formation.

Reaction Mechanism and Kinetics for Overall Reaction Rate

It is generally accepted that paraffin isomerization by Lewis acid catalysts proceeds through a chain mechanism involving a carbonium ion intermediate (*16*). The *n*-butane conversion on our catalyst melts would also proceed through the same mechanism. When the hydrogen chloride concentration is high at high temperatures, as in the case of our experimental conditions, the chain-initiating carbonium ion may be produced mainly by two processes (*16*). One is hydride ion abstraction from *n*-butane, accompanied by the formation of H_2, and the other is protolytic cracking of *n*-butane, accompanied by the formation of propane. In each case, dimeric Al_2Cl_6 acts as an electron acceptor and HCl is necessary as a proton source. The propane formation preceded by the isobutane suggests that the hydride ion abstraction may be a predominant process in the initiation step, though the formation of H_2 was not detected. The formation of C_3H_8 and i-C_5H_{12} may be explained by the disproportionation mechanism of the chain-initiating ion, a *t*-butyl ion (*19, 20*).

In the present study, only isobutane was formed in the absence of HCl. This result agreed qualitatively with that found by Pines and Wackher (*21*), who carried out the *n*-butane isomerization in a sealed glass reaction tube at 150°C. At high temperatures of about 150°C and in the absence of HCl, as suggested by Condon (*16*), a carbonium ion may be produced by a direct attack of aluminum chloride against *n*-butane, which leads to hydride ion abstraction from *n*-butane without formation of H_2.

We can rewrite Eq. (1) by considering the proportional relation between R and $P_{n\text{-B}}$ (Fig. 4),

$$R = k\left(A + \frac{K_{HCl}P_{HCl}}{1 + K_{HCl}P_{HCl}}\right)P_{n\text{-B}}, \quad (2)$$

where k is the rate constant. This equation may be derived by assuming that the rate-determining step is the formation of a chain-initiating ion on the melt surface. This assumption leads to the conclusion that R is equal to the sum of the rates of the initiation step in the presence and in the absence of HCl. Hydride ion abstraction from n-C_4H_{10}, with and without formation of H_2, corresponds to the above two initiation steps. Denoting the surface concentrations of HCl and n-C_4H_{10} by θ_{HCl} and $\theta_{n\text{-B}}$, and applying the Rideal mechanism to the initiation step in the presence of HCl, R can be expressed by

$$R = k_1P_{n\text{-B}}\theta_{HCl} + k_2\theta_{n\text{-B}}, \quad (3)$$

where k_1 and k_2 are the rate constants for each initiation step and it is assumed for the Rideal mechanism that interaction oc-

curs between adsorbed HCl and gaseous n-C_4H_{10}, even though some amount of n-C_4H_{10} is adsorbed. When the adsorption of both HCl and n-C_4H_{10} on the species Al_2Cl_6 is of a Langmuir type, one can write

$$\theta_{HCl} = \frac{K_{HCl}P_{HCl}}{1 + K_{HCl}P_{HCl} + K_{n-B}P_{n-B}}$$

and

$$\theta_{n-B} = \frac{K_{n-B}P_{n-B}}{1 + K_{HCl}P_{HCl} + K_{n-B}P_{n-B}}, \quad (4)$$

where K_{n-B} is the adsorption coefficient for n-C_4H_{10}. From Eqs. (3) and (4), we obtain

$$R = \frac{(k_1K_{HCl}P_{HCl} + k_2K_{n-B})P_{n-B}}{1 + K_{HCl}P_{HCl} + K_{n-B}P_{n-B}}. \quad (5)$$

Since, if n-C_4H_{10} is weakly adsorbed, $K_{n-B}P_{n-B}$ can be regarded as negligible, Eq. (5) becomes

$$R = \left[k_2K_{n-B} + \frac{(k_1 - k_2K_{n-B})K_{HCl}P_{HCl}}{1 + K_{HCl}P_{HCl}}\right]P_{n-B}. \quad (6)$$

Comparing Eq. (6) with (2), we have

$$k = k_1 - k_2K_{n-B} \quad \text{and} \quad A = \frac{k_2K_{n-B}}{k_1 - k_2K_{n-B}}; \quad (7)$$

k_2K_{n-B} is obtained by dividing R_0 in Fig. 3 by P_{n-B}. Furthermore, k_1 is evaluated from the intercept of the straight line in Fig. 9 with the ordinate, $1/(k_1 - k_2K_{n-B})P_{n-B}$, and K_{HCl} is obtained from the slope of the line, $1/(k_1 - k_2K_{n-B})P_{n-B}K_{HCl}$. The evaluated value of K_{HCl} at 150°C, 14 atm^{-1}, was much higher than literature values of 0.35 and 0.03 atm^{-1} for solid aluminum chloride supported by Al_2O_3 and SiO_2–Al_2O_3 at 60°C (*13*). By using these values, one can calculate the value of the term in the brackets on the right-hand side of Eq. (6). If Eq. (6) is acceptable, the value at 0.369 atm of P_{HCl} should agree with the slope of the straight line of R against P_{n-B} in Fig. 4. The value obtained from Eq. (6), 12.2×10^{-7} mol/min·cm²·atm, was indeed in excellent agreement with the slope in Fig. 4, 12.3×10^{-7}.

Temperature Dependence of Overall Reaction Rate

The observed maximum in R versus temperature (Fig. 7) will be discussed in this section. As the structural change of the catalyst melt does not occur over the temperature range studied (mp–160°C), as shown by the constant activation energy for the electric conduction (*22*), the cause of the maximum should be explained in terms of the reaction kinetics. The overall reaction rate, R, expressed by Eq. (6) can be rewritten as

$$R = \left(\frac{k_1K_{HCl}P_{HCl} + k_2K_{n-B}}{1 + K_{HCl}P_{HCl}}\right)P_{n-B}; \quad (8)$$

k_2K_{n-B} will be negligible compared with $k_1K_{HCl}P_{HCl}$ because the value of the former is less than 6% of the latter when $P_{HCl} = 0.369$ atm. Therefore, we find

$$R = \left(\frac{k_1K_{HCl}P_{HCl}}{1 + K_{HCl}P_{HCl}}\right)P_{n-B}. \quad (9)$$

Accordingly, the apparent activation energy E_a may be expressed as

$$E_a = E + (1 - \theta_{HCl})\Delta H_{HCl},$$

where E and ΔH_{HCl} are the true activation energy and the heat of adsorption of HCl, respectively (*13*). E_a is thus lower than E (>0) by $(1 - \theta_{HCl})\Delta H_{HCl}$ (<0). As the temperature is increased, θ_{HCl} at constant P_{HCl} decreases, that is, $(1 - \theta_{HCl})$ increases. Consequently E_a changes from a positive to a negative value, and a maximum in rate versus temperature is observed. The decrease in surface tension of the active species Al_2Cl_6 with temperature (*23*) may also contribute to the lowering of θ_{HCl}.

Difference in Catalytic Activity between the Molten and Solid States

The preceding discussion suggests that the n-butane conversion on our catalyst melts probably takes place on the melt surface and that the rate-controlling step

could be the carbonium ion formation in which the active species Al_2Cl_6 behaves as an electron acceptor. On the basis of this suggestion, the difference in catalytic activity between the molten and the solid states will now be discussed. The activity increased drastically at the melting point of a 61 mol% $AlCl_3$–39 mol% NaCl eutectic in spite of the lower actual surface area with the melt, and the overall reaction rate in the molten state was about 25 times that in the solid state. This finding is different from the result of Kenney and Takahashi (*9*) who found a smooth change in rate of dehydrochlorination of isopropyl chloride at the melting point of zinc chloride. The reason for the smooth change seems likely to be that the solid structure of $ZnCl_2$ is retained well above the melting point. The drastic increase in the activity observed in this work may be ascribed to the pronounced structural changes in aluminum chloride on melting. According to several reviews about the structure of aluminum chloride (*12, 24, 25*), the structure changes on fusion from an ionic crystal with a layer lattice to a molecular liquid consisting of a dimeric Al_2Cl_6 molecule. In other words, the change is from an ionic bonding, though partly covalent, to a covalent one. Since the presence of molecular species seems essential for the formation of carbonium ion, the variation from the ionic to the covalent state may increase markedly the catalytic activity at the melting point of the eutectic salt.

It was found that the change in the activity on passing from the molten to the supercooled state was continuous, in contrast to the discontinuous change from the supercooled to the solid state. The structure of the supercooled melt has not been found, but this finding suggests that the structure may be similar to that of the eutectic melt.

REFERENCES

1. Kenney, C. N., *Catal. Rev. Sci. Eng.* **11,** 197 (1975).
2. Riegel, H., Schindler, H. D., and Sze, M. C., *Chem. Eng. Progr.* **69**(10), 89 (1973).
3. Riegel, H., Schindler, H. D., and Sze, M. C., *Chem. Eng. N.Y.* **81**(13), 114 (1974).
4. Cover, A. E., Schreiner, W. C., and Skaperdas, G. T., *Chem. Eng. Progr.* **69**(3), 31 (1973).
5. Kohl, A. L., Harty, R. B., Johanson, J. G., and Naphtali, L. M., preprint, 85th National AIChE Meeting, 1978.
6. Ida, T., Nomura, N., Nakatsuji, Y., and Kikkawa, S., *Fuel,* **58,** 361 (1979).
7. Zielke, C. W., Klunder, E. B., Maskew, J. T., and Struck, R. T., *Ind. Eng. Chem. Process Des. Develop.* **19,** 85 (1980).
8. Bailey, R. A., and Prest, S. F., *Canad. J. Chem.* **49,** 1 (1971).
9. Kenney, C. N., and Takahashi, R., *J. Catal.* **22,** 16 (1971).
10. Butt, P. V., and Kenney, C. N., preprint, 6th International Congress on Catalysis, B17, 1976.
11. Ohtsuka, Y., and Tamai, Y., *J. Catal.* **51,** 169 (1978).
12. Boston, C. R., *in* "Advances in Molten Salt Chemistry" (J. Braunstein, G. Mamantov, and G. P. Smith, Eds.), Vol. 1, p. 129. Plenum, New York, 1971.
13. Oelderik, J. M., and Platteeuw, J. C., *in* "Proceedings, 3rd International Congress on Catalysis," Vol. 1, p. 736. North-Holland, Amsterdam, 1965.
14. Torsi, G., Mamantov, G., and Begun, G. M., *Inorg. Nucl. Chem. Lett.* **6,** 553 (1970).
15. Rytter, E., Oye, H. A., Cyvin, S. J., Cyvin, B. N., and Klaeboe, P., *J. Inorg. Nucl. Chem.* **35,** 1185 (1973).
16. Condon, F. E., *in* "Catalysis" (P. H. Emmett, Ed.), Vol. 6, p. 43. Reinhold, New York, 1958.
17. Narita, T., Ishikawa, T., and Midorikawa, R., *Denki Kagaku* (*J. Electrochem. Soc. Japan*) **36,** 749 (1968).
18. Narita, T., Ishikawa, T., and Midorikawa, R., *Denki Kagaku* (*J. Electrochem. Soc. Japan*) **36,** 300 (1968).
19. McCaulay, D. A., *J. Amer. Chem. Soc.* **81,** 6437 (1959).
20. Van Zijll Langhout, W. C., preprint 9th World Petroleum Congress, PD20(5), 1975.
21. Pines, H., and Wackher, R. C., *J. Amer. Chem. Soc.* **68,** 595 (1946).
22. Midorikawa, R., *Denki Kagaku* (*J. Electrochem. Soc. Japan*) **24,** 23 (1956).
23. Nisel'son, L. A., and Sokolova, T. D., *Russ. J. Inorg. Chem.* **10,** 827 (1965).
24. Semenenko, K. N., and Naumova, T. N., *Russ. J. Inorg. Chem.* **9,** 718 (1964).
25. Bigelow, N. J., *J. Chem. Educ.* **46,** 495 (1969).